ICAS 2016
30th Congress of the International Council of the Aeronautical Sciences
DCC, Daejeon, Korea ; September 25-30, 2016

SENSITIVITY ANALYSIS OF UNSTEADY AERODYNAMIC REDUCED-ORDER MODELS ROBUST TO FREESTREAM PARAMETER VARIATIONS

Maximilian Winter*, Christian Breitsamter*
***Technische Universität München, 85748 Garching, Germany**

Keywords: *Unsteady Aerodynamics, Reduced-Order Modeling, CFD, System Identification*

Abstract

In this paper, the sensitivity and performance of an unsteady aerodynamic reduced-order modeling (ROM) approach robust to freestream parameter variations is analyzed. The considered ROM methodology is founded on system identification principles and neurofuzzy networks in order to obtain an efficient aerodynamic model from CFD-based input-output data.

In terms of a sensitivity analysis, the user-defined parameters of the neurofuzzy model are varied systematically, while the ROM output for each set-up is compared with the full-order reference CFD solution. In this way, the influence of the ROM parameters is uncovered, while the focus is on a robustness and accuracy evaluation. Additionally, the number of freestream conditions incorporated within the training dataset is increased incrementally in order to study the dependence between the training information and the overall solution quality.

The research is carried out based on the NLR 7301 airfoil in the subsonic and transonic flight regime. It is shown that good agreement is obtained between the ROM results and the respective full-order solution. Moreover, the ROM parameters exhibit a robust characteristic which is beneficial for practical applications.

1 Introduction

The industrial design and analysis of next generation aircraft is characterized by involved multidisciplinary computations in order to achieve efficiency goals such as the reduction of emissions and fuel consumption. Based on these requirements, the aspect ratio of the wing tends to be increased, whereas it is envisioned to concurrently decrease the structural weight. Considering those highly-flexible structures, the accurate prediction of aeroelastic phenomena that arise through the interaction of structural, inertial, and flow-induced forces will become of even higher importance in the future. Hence, efficient and precise methods are required to compute the motion-induced aerodynamic forces. In this regard, the aim of the research efforts is to use modern CFD methods for the unsteady aerodynamic computations. However, due to the vast number of parameters, i.e., various freestream conditions, geometry parameters, fuel levels, etc., the numerical effort of comprehensive multi-physics calculations is still not manageable using the available computer technology.

A possible remedy is offered by the development and application of reduced-order models (see Lucia et al. [1] and Dowell and Hall [2] for instance). In this regard, computational-fluid-dynamics-based training samples describing the input/output relationship of the underlying system are exploited by means of an identification. In the context of unsteady aerodynamic computations, the system input is regarded with the structural and/or the rigid body degrees of freedom, whereas the outputs are the motion-induced generalized aerodynamic forces or aerodynamic coefficients. Following this methodology, the unsteady aerodynamic forces can be predicted with high accuracy, while the

simulations are performed within seconds once the ROM has been generated.

In the last years, a variety of linear and nonlinear ROM concepts have been developed to efficiently describe unsteady aerodynamic quantities. However, only a few approaches can be found in the literature that account for changing freestream conditions with a single ROM. Though, an efficient model that is valid across a range of inflow conditions is highly desirable for efficient simulation and control purposes. Thus, a brief description of the recently developed freestream-condition-adaptive ROM approaches is given below according to [3].

In 2010, a surrogate-based recurrence framework had been developed by Glaz et al. [4] in order to model the unsteady aerodynamic characteristics of rotor blades. Thereby, sinusoidal Mach number variations were taken into account, while a Kriging algorithm was used to train the ROM. Subsequently, Liu et al. [5] also employed a Kriging interpolation for the prediction of unsteady aerodynamic coefficients with respect to the NACA 64A010 airfoil undergoing a combined pitch and plunge motion at moderately changing freestream conditions. Recently, Winter and Breitsamter [3] developed a ROM based on neurofuzzy models which has been shown to yield good agreement for the generalized aerodynamic forces of the AGARD 445.6 wing across multiple Mach regimes ($0.5 \leq Ma_{\infty} \leq 1.2$). Nonetheless, it is still unclear how sensitive the formerly mentioned ROM approach responds to changes in the training data or model parameter variations.

In the present research, the ROM formulated by Winter and Breitsamter [3] is employed for a comprehensive sensitivity analysis. For this purpose, the NLR 7301 supercritical airfoil undergoing a pitching motion is considered across subsonic and transonic freestream conditions. The error estimation is realized by a comparison between the ROM output caused by harmonic excitations and the corresponding full-order CFD solution. In this regard, the influence of various ROM parameters is investigated systematically in order to obtain further insights about the robustness and accuracy of the method. Furthermore, several training data compositions with a varying number of freestream conditions is taken into account to obtain a ROM. In this way, the generalization capability of the model can be studied. Additionally, the question is addressed whether an increase in training information and trained flow conditions leads to a better overall simulation quality.

The paper is structured as follows: In Sec. 2, the employed inviscid CFD solver is explained briefly, whereas the ROM approach based on the local linear model tree algorithm (LOLIMOT, [6]) is discussed in Sec. 3. In Sec. 4, the NLR 7301 test case is introduced followed by the results and discussion of the sensitivity analysis. Finally, a conclusion in Sec. 5 summarizes the most important outcomes.

2 Computational Fluid Dynamics – Inviscid AER-Eu Solver

In the present work, the inviscid CFD solver AER-Eu is used to provide the neurofuzzy-network-based ROM with unsteady aerodynamic training data. Additionally, the AER-Eu solver developed at the Chair of Aerodynamics and Fluid Mechanics of the Technische Universität München (TUM-AER) is employed to compute the reference results required for error estimation.

AER-Eu solves the Euler equations by employing a shock-capturing finite-volume method for structured multi-block grids [7]. The spatial discretization is realized by Roe's flux-difference splitting, while the monotonic upstream scheme for conservation laws (MUSCL) extrapolation is used to retain the total variation diminishing (TVD) property. The temporal integration is realized with the implicit dual-time-stepping scheme, whereas the embedded pseudo-time iterations are carried out using the lower-upper symmetric successive over-relaxation (LU-SSOR). Furthermore, a mesh deformation algorithm has been implemented. In this context, a user-defined time law can be prescribed to interpolate between a reference grid and various amplitude grids. For further information, refer to Refs. 7-10.

3 Aerodynamic Reduced-Order Model

The aerodynamic ROM proposed in Winter and Breitsamter [3] utilizes the LOLIMOT algorithm developed by Nelles [6] to train the dynamic relationship between the structural excitation, the freestream parameters, and the corresponding unsteady aerodynamic loads. In order to support the following theoretical presentation, an overview of the ROM training and application process is depicted in Fig. 1, while the nomenclature is adapted to support the investigations of this work. The basic concept for the aerodynamic ROM is the external dynamics approach (or recurrence framework method). Thereby, it is assumed that the output of the considered system can be approximated by means of current and previous excitation inputs as well as previous system responses [11]. Considering for example the aerodynamic lift coefficient C_L as the system output and the angle of incidence α in combination with the freestream Mach number Ma_∞ as the system input, the modeling framework can be written as:

$$\hat{C}_L(k) = \mathcal{N}\left[\begin{pmatrix}\alpha(k)\\ \alpha(k-1)\\ \vdots\\ \alpha(k-m)\end{pmatrix}, Ma_\infty, \begin{pmatrix}C_L(k-1)\\ C_L(k-2)\\ \vdots\\ C_L(k-n)\end{pmatrix}\right] \quad (1)$$

$$\hat{C}_L(k) = \mathcal{N}(\boldsymbol{u}), \qquad \boldsymbol{u} \in \mathbb{R}^p$$

In Eq. (1), k denotes the current discrete-time increment, i.e., $\tau(k+1) = \tau(k) + \Delta\tau$, while the predicted lift coefficient is characterized by $\hat{C}_L$. It should be noted that the same methodology also applies for other output quantities as well. Moreover, m and n are introduced in Eq. (1) as the maximum dynamic delay-orders for the angle of attack and the lift coefficient, respectively. Since these parameters have to be determined a priori by the user, they are considered within the sensitivity and robustness investigation.

When combining Eq. (1) with a nonlinear approximator in terms of the unknown function $\mathcal{N}$, the nonlinear auto-regressive with exogenous input (NARX, [6]) model architecture is obtained. In this context, the neurofuzzy model from the domain of artificial neural networks is employed to approximate $\mathcal{N}$ based on a given training example. The basic concept of local linear neurofuzzy models consists in the superposition and blending of various local linear models (LLMs) which are valid in certain regimes of the model input space. Moreover, the input space assignment for the LLMs is achieved via fuzzy validity functions.

According to Nelles [6], the basis function formulation for a neurofuzzy model with M LLMs can be expressed as:

$$\hat{C}_L = \sum_{j=1}^{M}\left[w_{j0} + w_{j1}u_1 + \cdots + w_{jp}u_p\right]\Psi_j(\boldsymbol{u}) \quad (2)$$

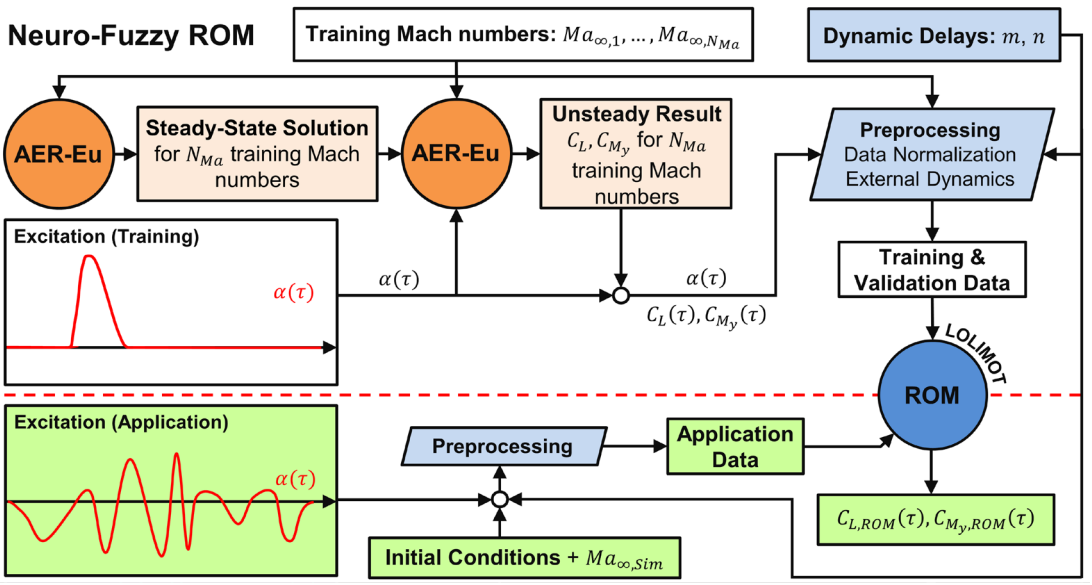

Fig. 1. Overview of the aerodynamic ROM approach considered for the sensitivity analysis.

In Eq. (2), the coefficients w_{jl} represent the linear model weights, whereas u_l characterizes the lth element of the network input vector $\boldsymbol{u}$. Besides, Ψ_j refers to the fuzzy validity function of the jth LLM. Each validity function is composed of normalized Gaussians evaluated with the Euclidean distance between the network input vector and the center of the respective LLM [3]. Thereby, the constant k_σ has to be defined by the user in order to determine the range of influence for the local linear models (see also Nelles [6]). If k_σ is chosen too small, the influence of the LLMs is limited to the vicinity of their center. In contrast, if k_σ is chosen too large, each LLM affects adjacent local linear models disproportionately high. Both effects are undesirable. For this reason, the parameter k_σ is investigated in further detail in Sec. 4.4.

For the determination of the various unknowns occurring in Eq. (2), a training dataset must be provided. Therefore, an unsteady forced-motion CFD computation has to be performed yielding the correlated time series of the system's inputs and outputs. Here, different inflow conditions are considered by means of several freestream Mach numbers Ma_∞. Hence, the CFD-based data has to be generated at N_{Ma} different supporting points (see Fig. 1). As the parameter N_{Ma} as well as the distribution of the training Mach numbers Ma_{Trn} have a crucial influence on the ROM performance, the sensitivity with respect to the selection of training conditions is also a subject of this paper.

Subsequent to the preprocessing steps shown in Fig. 1, the data provided by the AER-Eu solver can be utilized to train the neurofuzzy model using the LOLIMOT algorithm. Since a detailed review of the LOLIMOT training procedure is beyond the scope of this work, the reader is referred to Nelles [6] and Winter and Breitsamter [3] for a thorough discussion.

4 Sensitivity Analysis

In this section, the ROM approach is applied to the NLR 7301 airfoil undergoing a pitching motion in order to investigate the method's sensitivity, robustness, and accuracy. Therefore, various aerodynamic ROMs are considered, which represent different parameter set-ups and training data configurations. After the efficient models have been calibrated, they are utilized to produce the aerodynamic response, i.e., the lift (C_L) and pitching moment (C_{M_y}) coefficient time series, induced by harmonic pitching oscillations at several reduced frequencies. Analogously to the common practice within the aeroelastic community, the time domain unsteady aerodynamic data resulting from the harmonic excitations are transferred into the frequency domain via Fourier analysis for both the ROM and the CFD reference data. The error estimation is then performed in terms of a comparison between the ROM output and the corresponding full-order CFD solution.

4.1 Test Case Description: NLR 7301 Airfoil

The well-known NLR 7301 supercritical airfoil [12, 13] is governed by a distinct nonlinear aerodynamic behavior in the transonic flight regime due to the presence of a strong shock on the airfoil's suction side, which can be proven by the steady pressure coefficient distribution in Fig. 2. The airfoil is characterized by a chord length of $c = 0.3\ m$, which serves also as the reference length for the reduced frequency calculation given in Eq. (3).

$$k_{red} = \frac{\omega \cdot c}{U_\infty} \tag{3}$$

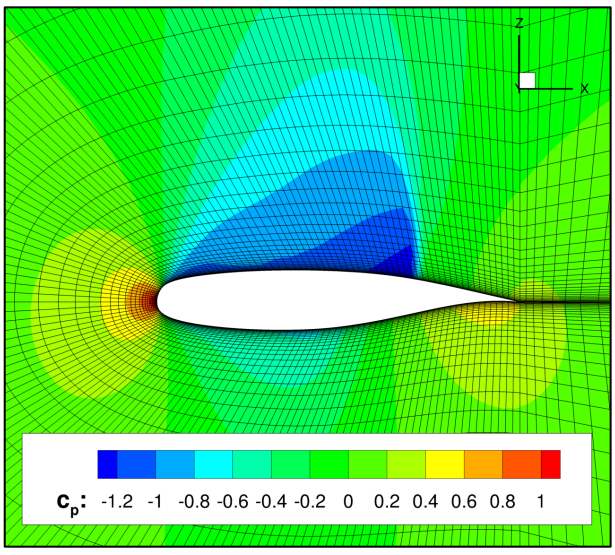

Fig. 2. Structured reference grid and computed steady-state pressure coefficient distribution of the NLR 7301 airfoil at $Ma_\infty = 0.75$ and $\alpha_0 = 0°$ (AER-Eu).

The employed computational grid also shown in Fig. 2 is composed of 14,396 cells in a four-block C-H topology using ANSYS ICEM CFD. Moreover, a grid sensitivity study was carried out in [14] to ensure the independence of the solution from the grid resolution. Since the focus in this work is exclusively on an intermethod comparison, the considered Mach numbers are chosen independently from the experimental test conditions regarded in [12]. In the following, the freestream Mach number range of $0.5 \leq Ma_\infty \leq 0.9$, resolved with $\Delta Ma_\infty = 0.05$, is considered, while the steady angle of incidence is fixed at $\alpha_0 = 0°$. The freestream conditions, therefore, range from the subsonic to the transonic flow regimes. In Fig. 3, the steady-state lift and pitching moment coefficients are plotted against Ma_∞ to emphasize their nonlinear characteristic with respect to the NLR 7301 test case. Therefore, the intended study can be considered as a challenging task for the freestream-parameter-adaptive ROM.

4.2 Training Data Generation

Starting from the steady-state solutions, the unsteady AER-Eu-based flow computations have been carried out to obtain the transient responses of the aerodynamic system for the selected freestream conditions. Therefore, a maximum pitching angle amplitude of $\alpha^1 = 0.01°$ is chosen to restrict the nonlinear dependencies to the variations in the freestream Mach number. Henceforth, dynamic linearity around the nonlinear reference states is assumed by considering only small amplitudes (see also [3]).

In order to generate the ROM training data according to the workflow depicted in Fig. 1, the so-called pulse signal suggested by Kaiser et al. [15] is employed in this work for the excitation of the pitching degree of freedom. In contrast to the amplitude-modulated pseudo-random binary signal (APRBS), which has been originally used within the training procedure for generality [3], the pulse signal is well-suited for dynamically linear identification purposes.

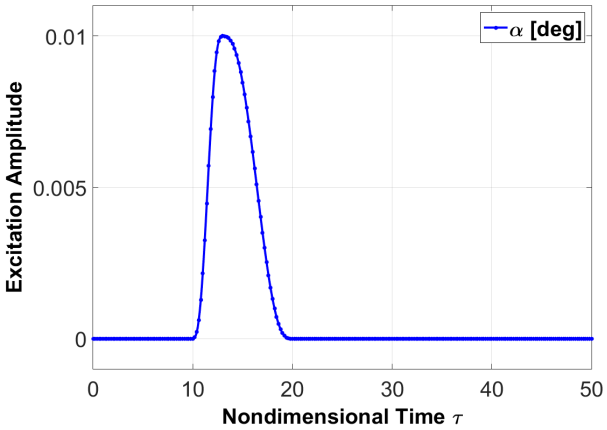

Fig. 4. Discrete-time series of the pulse signal [15] for the forced-motion excitation of the NLR 7301 pitching degree of freedom.

In this context, a nondimensional time step size of $\Delta\tau = 0.1$ and a pulse length of 100 time steps are utilized as shown in Fig. 4. For convenience, the same signal is used for the N_{Ma} unsteady computations. As a result of the AER-Eu simulations, the ROM training data are obtained.

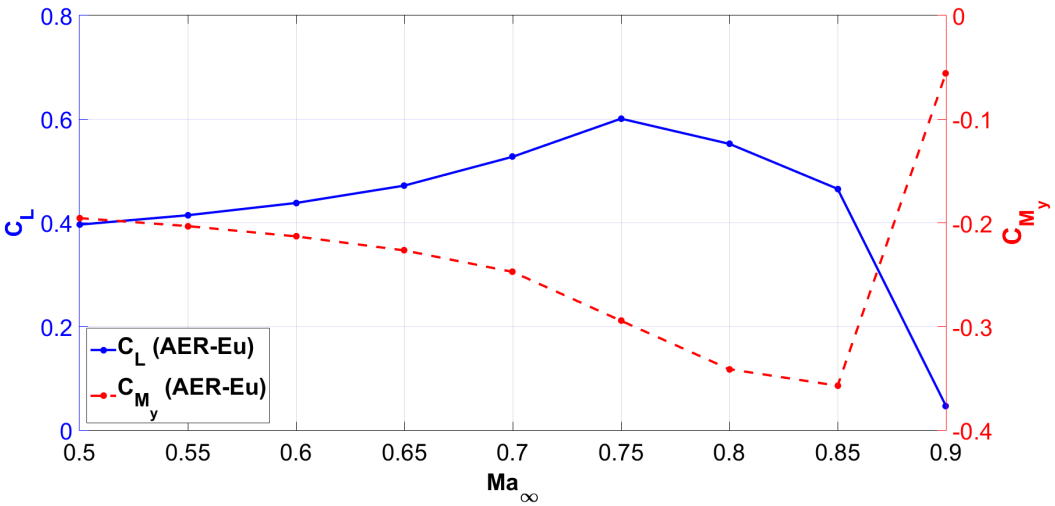

Fig. 3. Development of the steady aerodynamic coefficients as a function of Ma_∞ (NLR 7301, $\alpha_0 = 0°$).

4.3 Sensitivity to ROM Parameter Variations

For the sensitivity study regarding the ROM parameters, only the training dataset composed of five freestream Mach numbers ($N_{Ma} \equiv 5$) is taken into account. According to Table 1, the trained freestream conditions marked with the letter 'X' can be read as $Ma_{Trn} = [0.5, 0.6, 0.7, 0.8, 0.9]$. Thus, the pulse excitation signal and the respective aerodynamic response evaluated at five Ma_{Trn} are employed to train the ROM. Nevertheless, the application to harmonic pitching oscillations is always performed for all $N_{Ma} = 9$ cases (see Table 1) as well as the five reduced frequencies listed in Table 2. In order to achieve load periodicity, three oscillation cycles are computed with the ROM and the AER-Eu solver [3, 9]. For the latter method, each cycle is resolved with 100 time steps. In contrast, the ROM is applied with a constant time step size ($\Delta\tau = 0.1$) leading to a frequency-dependent cycle discretization. In the present work, the error between the ROM and the CFD reference is measured by the mean squared error (MSE). For example, the MSE with respect to the real part of the first harmonic lift coefficient ($Re\ C_L^1$) is defined by

$$MSE(Re\ C_L^1) = \frac{1}{9 \cdot 5} \sum_{i=1}^{9} \sum_{j=1}^{5} \left[Re\ C_{L,ROM}^1(Ma_{\infty,i}, k_{red,j}) - Re\ C_{L,CFD}^1(Ma_{\infty,i}, k_{red,j}) \right]^2 \quad (4)$$

Ma_∞ ------ N_{Ma}	0.5	0.55	0.6	0.65	0.7	0.75	0.8	0.85	0.9
2	X								X
3	X				X				X
4	X				X		X		X
5	X		X		X		X		X
6	X		X		X	X	X		X
7	X		X		X	X	X	X	X
8	X		X	X	X	X	X	X	X
9	X	X	X	X	X	X	X	X	X

Tab. 1: Overview of the training Mach number compositions considered for the ROM training.

Hence, the error can be determined consistently for the frequency domain first harmonic lift and pitching moment coefficients at various model set-ups. Based on the previously described modus operandi, the sensitivity analysis has been conducted.

k_{red}	0.05	0.10	0.20	0.40	0.60
ROM	X	X	X	X	X
AER-Eu	X	X	X	X	X

Tab. 2: Overview of the reduced frequencies computed with the ROM and the AER-Eu solver.

Firstly, the maximum input delay-order (m) is varied in the range of $1 \leq m \leq 18$, whereas the maximum output delay-order is fixed at $n = 1$. Moreover, k_σ is chosen to be 0.5. The result of this analysis is visualized in Fig. 5. The diagram indicates an optimal range for m between 2 and 9, where the lowest ROM-based error is observed. However, the error increases again if m is chosen too large (here, if $m > 9$).

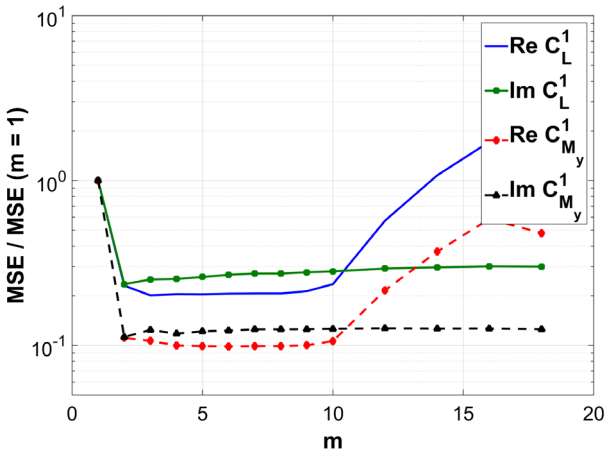

Fig. 5. Evaluation of the mean squared error with respect to varying maximum input delay-orders (NLR 7301, $\alpha_0 = 0°$, $\alpha^1 = 0.01°$, $n = 1$, $k_\sigma = 0.5$, $N_{Ma} = 5$).

Secondly, the maximum output delay-order (n) is modified in the range of $1 \leq n \leq 20$, whereas the maximum input delay-order is fixed at $m = 5$. The resulting error characteristics are plotted in Fig. 6. Based on these results, no clear trend can be discovered. The minimum error considering the real and imaginary parts of both aerodynamic coefficients is achieved at $n = 1$.

Since it is difficult to derive general user guidelines based on the information from Figs. 5 and 6, another sensitivity study has been performed. In the following, both maximum delay-orders, namely m and n, are varied simultaneously, while the condition $m = n$ applies. Fig. 7 depicts the outcome of this analysis. In contrast to the previous considerations, a saturation is ascertained for larger maximum output delays, which is beneficial for practical purposes.

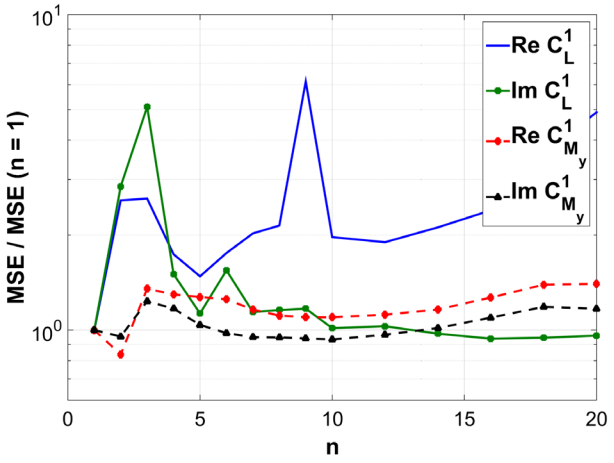

Fig. 6. Evaluation of the mean squared error with respect to varying maximum output delay-orders (NLR 7301, $\alpha_0 = 0°$, $\alpha^1 = 0.01°$, $m = 5$, $k_\sigma = 0.5$, $N_{Ma} = 5$).

In Fig. 7, the solution accuracy remains nearly unchanged for m and n larger than ~10. Hence, the quality of the results is not improved with more considered delay-elements whereas the required computational effort for training and applying the ROM is increased. The important conclusion is, on the one hand, that relatively small maximum input and output delay-orders (in the range of 3 to 12) are sufficient for an adequate approximation of the system characteristics. On the other hand, if m and n are chosen too large, the accuracy is not negatively affected in contrast to the numerical cost.

Furthermore, the influence of the neurofuzzy model parameter k_σ has been investigated (see Sec. 3). For this purpose, the training data characterized by $N_{Ma} = 5$ (cf. Table 1) is used to train the model. Moreover, the maximum input and output delays, which have been analyzed beforehand, are set to $m = n = 10$. In Fig. 8, the resulting mean squared error is plotted over the factor k_σ, while this model parameter has been varied in the range of $0.2 \leq k_\sigma \leq 0.95$.

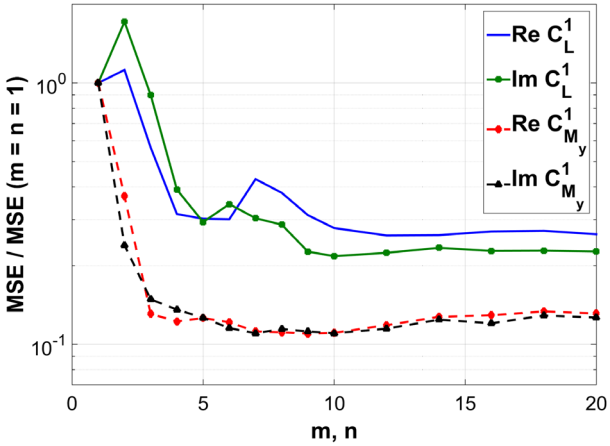

Fig. 7. Evaluation of the mean squared error with respect to simultaneously varying maximum delay-orders (NLR 7301, $\alpha_0 = 0°$, $\alpha^1 = 0.01°$, $m = n$, $k_\sigma = 0.5$, $N_{Ma} = 5$).

For $k_\sigma < 0.2$, no solution has been obtained because the influence regime of the LLMs becomes to small. As can be seen in Fig. 8, the optimal range for k_σ is between 0.2 and 0.5. Considering higher k_σ, the error is abruptly increased, which applies especially for the real parts of the aerodynamic coefficients. Interestingly, the imaginary parts are almost not affected by this trend. Nonetheless, for practical purposes, the parameter k_σ should be selected in the range of $0.25 \leq k_\sigma \leq 0.5$.

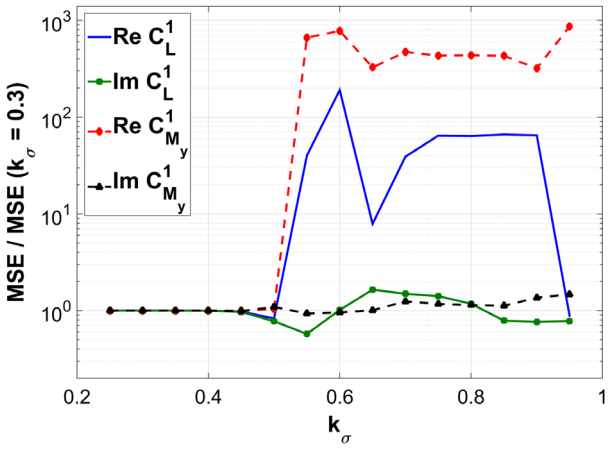

Fig. 8. Evaluation of the mean squared error with respect to a variation of the neurofuzzy model parameter k_σ (NLR 7301, $\alpha_0 = 0°$, $\alpha^1 = 0.01°$, $m = 10$, $n = 10$, $N_{Ma} = 5$).

4.4 Sensitivity to Training Data Variations

Additionally, a sensitivity analysis with respect to the training data has been conducted. Therefore, the model parameters considered in the previous subsection are fixed to $m = 10, n = 10$, and $k_\sigma = 0.5$. In the following, the number of freestream conditions incorporated within the training dataset (N_{Ma}) is varied (see Table 1), although the application is still performed for all freestream conditions, i.e., $N_{Ma} = 9$. In this way, the generalization capability of the ROM with respect to Ma_∞ can be studied.

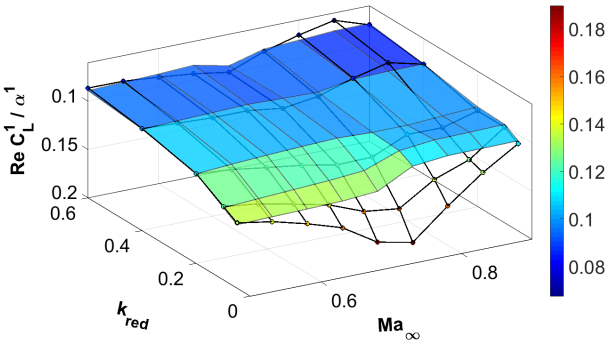

Fig. 9. Real (Re) part of the first harmonic of C_L as a function of k_{red} and Ma_∞ (NLR 7301, $\alpha_0 = 0°$, $\alpha^1 = 0.01°$, $m = 10$, $n = 10$, $k_\sigma = 0.5$, $Ma_{Trn} = [0.5, 0.9]$, ROM = Surface, AER-Eu = Lattice).

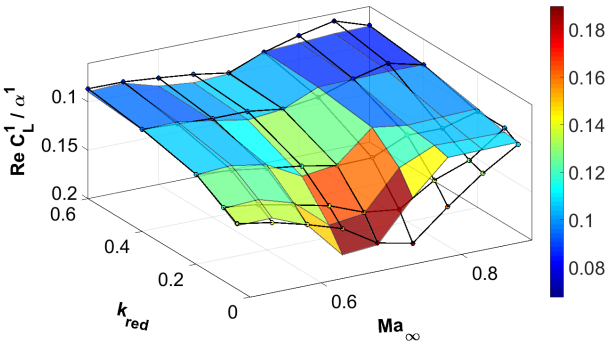

Fig. 10. Real (Re) part of the first harmonic of C_L as a function of k_{red} and Ma_∞ (NLR 7301, $\alpha_0 = 0°$, $\alpha^1 = 0.01°$, $m = 10$, $n = 10$, $k_\sigma = 0.5$, $Ma_{Trn} = [0.5, 0.7, 0.9]$, ROM = Surface, AER-Eu = Lattice).

Figures 9-12 show the results of this investigation regarding the real part of the first harmonic of the lift coefficient, which is plotted against the reduced frequency and the freestream Mach number. Thereby, the ROM results are characterized by the surface plot, whereas the AER-Eu solution is represented by the lattice.

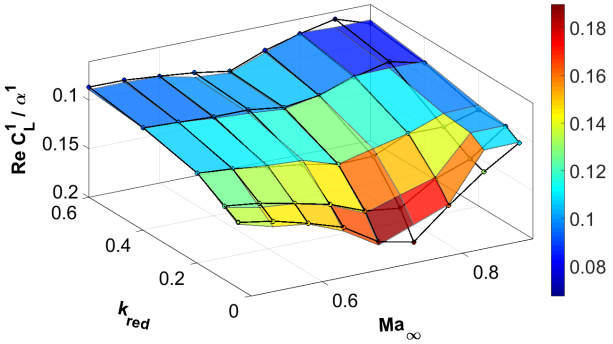

Fig. 11. Real (Re) part of the first harmonic of C_L as a function of k_{red} and Ma_∞ (NLR 7301, $\alpha_0 = 0°$, $\alpha^1 = 0.01°$, $m = 10$, $n = 10$, $k_\sigma = 0.5$, $Ma_{Trn} = [0.5, 0.6, 0.7, 0.8, 0.9]$, ROM = Surface, AER-Eu = Lattice).

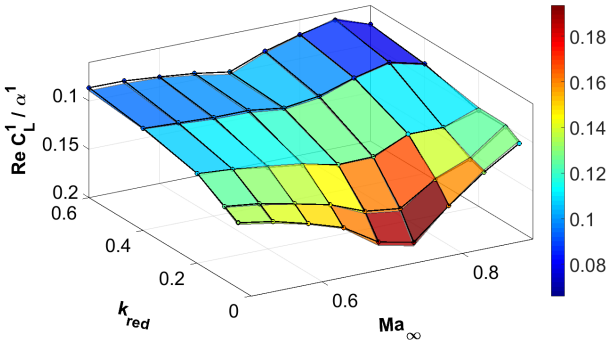

Fig. 12. Real (Re) part of the first harmonic of C_L as a function of k_{red} and Ma_∞ (NLR 7301, $\alpha_0 = 0°$, $\alpha^1 = 0.01°$, $m = 10$, $n = 10$, $k_\sigma = 0.5$, $Ma_{Trn} = [0.5, 0.6, 0.65, 0.7, 0.75, 0.8, 0.85, 0.9]$, ROM = Surface, AER-Eu = Lattice).

As can be demonstrated by Figs. 9-12, the ROM is able to reproduce the freestream conditions contained in the training dataset with a predominantly good to very good agreement. With an increasing level of training information, i.e., for larger N_{Ma}, the solution quality is improved continuously. In Fig. 12, aside from a very slight offset, a very good agreement is ascertained, which holds true for the reduced frequency as well as the freestream Mach number. However, as it has been already noted by Winter and Breitsamter [3], only the characteristics that have been trained by the ROM can be reproduced adequately. Hence, a finer Mach number resolution is typically required for the transonic flight regime. Nonetheless, it is demonstrated that a ROM trained with a sufficient number of freestream conditions can accurately reproduce the nonlinear characteristics of the unsteady aerodynamic loads.

The ROM-generated real and imaginary parts of the pitching moment coefficient depicted in Figs. 13-15 show the same trend as discussed for the lift coefficient. Hence, a very good correlation is obtained between the ROM results and the reference solution (AER-Eu) regarding the trained freestream conditions.

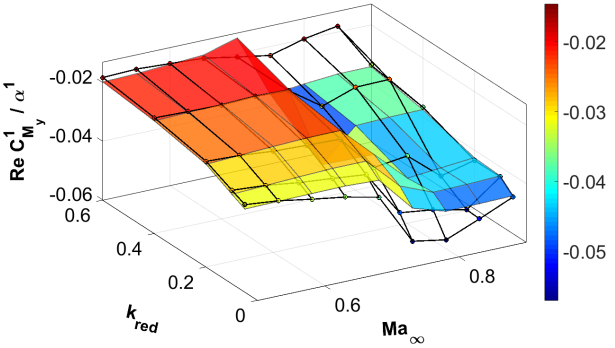

Fig. 13. Real (Re) part of the first harmonic of C_{M_y} as a function of k_{red} and Ma_∞ (NLR 7301, $\alpha_0 = 0°$, $\alpha^1 = 0.01°$, $m = 10$, $n = 10$, $k_\sigma = 0.5$, $Ma_{Trn} = [0.5, 0.9]$, ROM = Surface, AER-Eu = Lattice).

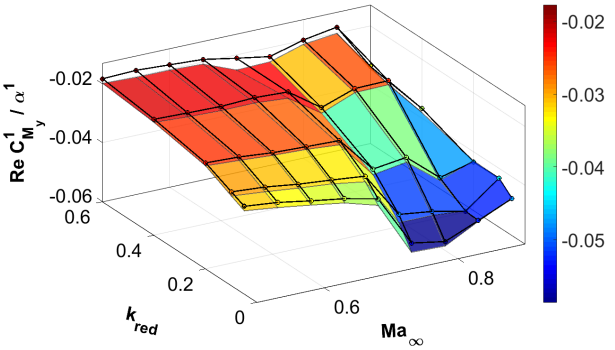

Fig. 14. Real (Re) part of the first harmonic of C_{M_y} as a function of k_{red} and Ma_∞ (NLR 7301, $\alpha_0 = 0°$, $\alpha^1 = 0.01°$, $m = 10$, $n = 10$, $k_\sigma = 0.5$, $Ma_{Trn} = [0.5, 0.6, 0.65, 0.7, 0.75, 0.8, 0.85, 0.9]$, ROM = Surface, AER-Eu = Lattice).

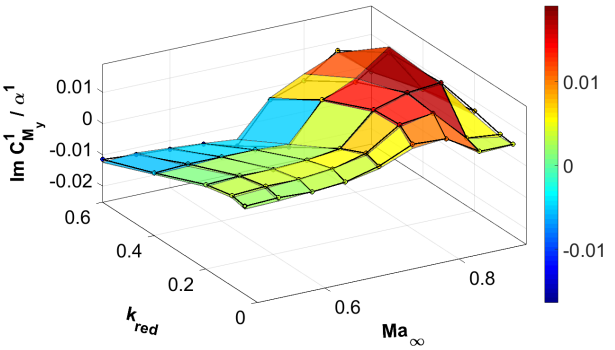

Fig. 15. Imaginary (Im) part of the first harmonic of C_{M_y} as a function of k_{red} and Ma_∞ (NLR 7301, $\alpha_0 = 0°$, $\alpha^1 = 0.01°$, $m = 10$, $n = 10$, $k_\sigma = 0.5$, $Ma_{Trn} = [0.5, 0.6, 0.65, 0.7, 0.75, 0.8, 0.85, 0.9]$, ROM = Surface, AER-Eu = Lattice).

In order to consider the ROM's generalization behavior in more detail, the results at a reduced frequency of $k_{red} = 0.4$ are extracted and shown in Figs. 16 and 17. Similar to the prior observations, a better agreement is ascertained for the subsonic conditions than for the transonic flight regime if the number of considered training Mach numbers is low ($N_{Ma} < 5$). Nonetheless, the overall prediction quality of the ROM is good as the general trend can be reproduced even with a non-optimal model, i.e., a model trained by an insufficient number of freestream conditions.

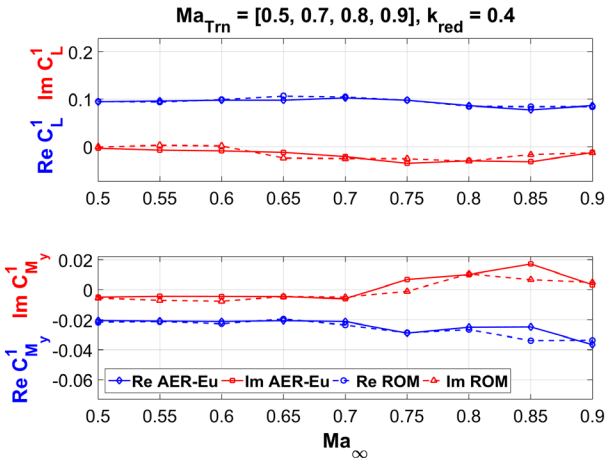

Fig. 16. Real (Re) and imaginary (Im) parts regarding C_L and C_{M_y} as a function of the freestream Mach number (NLR 7301, $\alpha_0 = 0°$, $\alpha^1 = 0.01°$, $m = 10$, $n = 10$, $k_\sigma = 0.5$, $N_{Ma} = 4$, $k_{red} = 0.4$).

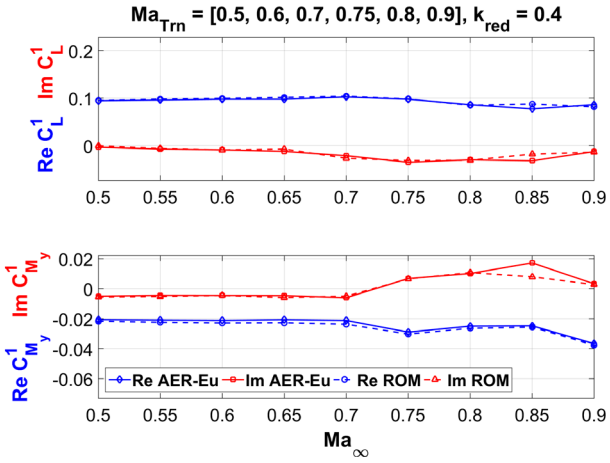

Fig. 17. Real (Re) and imaginary (Im) parts regarding C_L and C_{M_y} as a function of the freestream Mach number (NLR 7301, $\alpha_0 = 0°$, $\alpha^1 = 0.01°$, $m = 10$, $n = 10$, $k_\sigma = 0.5$, $N_{Ma} = 6$, $k_{red} = 0.4$).

Finally, the mean squared error defined in Eq. (4) is also evaluated in terms of the training data

sensitivity analysis. The resulting diagram shows the development of the ROM error in terms of a variation of the number of considered freestream conditions N_{Ma} (see also Table 1).

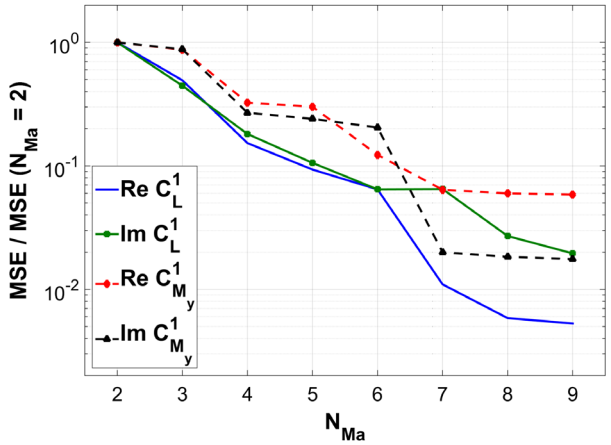

Fig. 18. Evaluation of the mean squared error with respect to a variation of N_{Ma} according to Table 1 (NLR 7301, $\alpha_0 = 0°$, $\alpha^1 = 0.01°$, $m = 10$, $n = 10$, $k_\sigma = 0.5$).

Figure 18 indicates that the incorporation of more training information leads to a better overall model-based prediction.

5 Conclusions

In the present paper an unsteady aerodynamic reduced-order modeling approach valid to freestream parameter variations has been recapitulated and, subsequently, applied to a numerical test case in order to investigate the sensitivity of the model. On the one hand, the model parameters, namely the maximum dynamic delay-orders and the constant k_σ of the neurofuzzy model, have been varied systematically. It was shown that an optimal range exists for the model parameters, enabling a robust application of the model for practical purposes.

On the other hand, several training data configurations with a varying number of freestream conditions was taken into account. It was demonstrated that a ROM trained with a sufficient number of freestream conditions can reproduce the associated unsteady air loads with high accuracy. Furthermore, it was shown that the incorporation of more training information leads to a better overall prediction quality.

Besides, the numerical effort was reduced by a factor of 79.2 for the investigated test case, although the same parameter space was considered for the ROM and the CFD reference. It has to be emphasized that an established ROM can be employed for other reduced frequencies, excitation types, and freestream Mach numbers. Hence, the speed-up factor could be even higher for non-academic considerations.

Acknowledgments

The authors would like to thank the Bavarian Research Foundation (Bayerische Forschungsstiftung) for the funding of the project ROM-Aer (AZ 1050-12).

Contact Author Email Address

mailto: maximilian.winter@aer.mw.tum.de

References

[1] Lucia D. J., King P. I., and Beran P. S. Reduced-order modeling of a two-dimensional flow. *Computers & Fluids*, Vol. 32, pp 917–938, 2003.

[2] Dowell E. H. and Hall K. C., Modeling of fluid-structure interaction. *Annual Review of Fluid Mechanics*, Vol. 33, pp 445-490, 2001.

[3] Winter M. and Breitsamter C. Neurofuzzy-model-based unsteady aerodynamic computations across varying freestream conditions. *AIAA Journal*, 2016.

[4] Glaz B., Liu L., and Friedmann P. P. Reduced-order nonlinear unsteady aerodynamic modeling using a surrogate-based recurrence framework. *AIAA Journal*, Vol. 48, No. 10, pp 2418-2429, 2010.

[5] Liu H., Hu H., Zhao Y., and Huang R. Efficient reduced-order modeling of unsteady aerodynamics robust to flight parameter variations. *Journal of Fluids and Structures*, Vol. 49, pp 728-741, 2014.

[6] Nelles O. *Nonlinear system identification - from classical approaches to neural networks and fuzzy models*, Springer, 2001.

[7] Kreiselmaier E. and Laschka B. Small disturbance Euler equations: efficient and accurate tool for unsteady load predictions. *Journal of Aircraft*, Vol. 37, No. 5, pp 770-778, 2000.

[8] Pechloff A. and Laschka B. Small disturbance Navier–Stokes method: efficient tool for predicting unsteady air loads. *Journal of Aircraft*, Vol. 43, No. 1, pp 17-29, 2006.

[9] Fleischer D. and Breitsamter C. Efficient computation of unsteady aerodynamic loads using computational-fluid-dynamics linearized methods. *Journal of Aircraft*, Vol. 50, No. 2, pp 425-440, 2013.

[10] Förster M. and Breitsamter C. Aeroelastic prediction of discrete gust loads using nonlinear and time-linearized CFD-methods. *Journal of Aeroelasticity and Structural Dynamics*, Vol 3, No 3, pp 19-38, 2015.

[11] Ljung L. *System identification: theory for the user*, Prentice-Hall, 1987.

[12] Schewe G. and Deyhle H. Experiments on transonic flutter of a two-dimensional supercritical wing with emphasis on the non-linear effects. *Proceedings of the Royal Aeronautical Society Conference on Unsteady Aerodynamics*, London, U.K., 1996.

[13] Tang L., Bartels R. E., Chen P.-C., and Liu D. D. Numerical investigation of transonic limit cycle oscillations of a two-dimensional supercritical wing. *Journal of Fluids and Structures*, Vol. 17, No. 1, pp 29-41, 2003.

[14] Winter M. and Breitsamter C. Reduced-order modeling of unsteady aerodynamic loads using radial basis function neural networks. *63rd Deutscher Luft- und Raumfahrtkongress*, Augsburg, Germany, DGLR Paper 2014-340013, 2014.

[15] Kaiser C., Thormann R., Dimitrov D., and Nitzsche J. Time-linearized analysis of motion-induced and gust-induced airloads with the DLR TAU code. *64th Deutscher Luft- und Raumfahrtkongress*, Rostock, Germany, DGLR Paper 2014-370189, 2015.

Copyright Statement